Cell

Deregulation of Scribble Promotes Mammary Tumorigenesis and Reveals a Role for Cell Polarity in Carcinoma

Lixing Zhan,[1] Avi Rosenberg,[1,2] Kenneth C. Bergami,[1] Min Yu,[1] Zhenyu Xuan,[1] Aron B. Jaffe,[3] Craig Allred,[4] and Senthil K. Muthuswamy[1,*]

[1]Cold Spring Harbor Laboratory, Watson School of Biological Sciences, One Bungtown Road, Cold Spring Harbor, NY 11724, USA
[2]Program in Genetics, Stony Brook University, Stony Brook, NY 11794, USA
[3]Cell Biology Program, Memorial Sloan-Kettering Institute, New York, NY 10021, USA
[4]Department of Pathology and Immunology, Washington University School of Medicine, St. Louis, MO 63110, USA
*Correspondence: muthuswa@cshl.edu
DOI 10.1016/j.cell.2008.09.045

SUMMARY

Loss of cell polarity proteins such as Scribble induces neoplasia in *Drosophila* by promoting uncontrolled proliferation. In mammals, the role that polarity proteins play during tumorigenesis is not well understood. Here, we demonstrate that depletion of Scribble in mammary epithelia disrupts cell polarity, blocks three-dimensional morphogenesis, inhibits apoptosis, and induces dysplasia in vivo that progress to tumors after long latency. Loss of Scribble cooperates with oncogenes such as *c-myc* to transform epithelial cells and induce tumors in vivo by blocking activation of an apoptosis pathway. Like depletion, mislocalization of Scribble from cell-cell junction was sufficient to promote cell transformation. Interestingly, spontaneous mammary tumors in mice and humans possess both downregulated and mislocalized Scribble. Thus, we demonstrate that *scribble* inhibits breast cancer formation and that deregulation of polarity pathways promotes dysplastic and neoplastic growth in mammals by disrupting morphogenesis and inhibiting cell death.

INTRODUCTION

Breast cancer is thought to originate from epithelial cells of the terminal ductal lobular units (TDLU) in the breast (Allred et al., 2001, 2004). Each TDLU has multiple small units referred to as acini that consist of a single polarized layer of luminal epithelial cells surrounding a hollow lumen (Allred et al., 2001; Bissell et al., 2002; Rodriguez-Boulan and Nelson, 1989). The establishment and maintenance of polarized organization is critical for normal function of mammary epithelial cells in vivo. Early during initiation and progression of carcinoma, epithelial cells lose their ability to maintain a normal polarized organization, suggesting a critical role for molecules that regulate cell polarity in breast cancer.

Establishment of apical-basal polarity in mammalian epithelia is coordinated by a set of proteins referred to as polarity regulators (Nelson, 2003). These include the Scribble (Scrib)/lethal (2) giant larvae (Lgl)/discs large (Dlg) proteins that direct formation of basolateral membranes and the Crumbs/PALS/PATJ and partitioning defective 3 (Par3)/Par6/atypical protein kinase C (aPKC) protein complexes that direct establishment of the apical membrane and the apical-basal border, respectively (Macara, 2004; Margolis and Borg, 2005; Nelson, 2003).

In *Drosophila*, loss of function mutations in polarity genes such as *scrib, lgl, and dlg1* result in aberrant proliferation and abnormal cell polarity/architecture, demonstrating a direct relationship between cell polarity regulators and control of cell proliferation (Bilder, 2004; Bryant, 1997). Although the mechanistic details of the relationship between polarity and cell proliferation is not well understood, genetic analysis suggests that polarity proteins use separate pathways to regulate cell structure and cell proliferation (Lorenzo et al., 1999).

Recent studies suggest a role for polarity proteins in human cancers. For example, human Scribble and DLG1 are targeted for ubiquitin-mediated proteolysis by the E6 oncoprotein from high-risk strains of human papillomavirus (HPV) (Gardiol et al., 1999; Humbert et al., 2003; Nakagawa and Huibregtse, 2000). Genetic alteration in *dlg5* is correlated with inflammatory bowel disease, which predisposes the patient to gastric cancer (Stoll et al., 2004). Furthermore, loss of *scrib* expression is frequently observed in colon and lobular breast cancers (Gardiol et al., 2006; Navarro et al., 2005). In addition, we recently demonstrated that the oncogene ErbB2 requires an interaction with the Par6/aPKC polarity complex to transform three-dimensional (3D) mammary epithelial acini (Aranda et al., 2006). These findings indicate an important role for polarity proteins during cell transformation. However, neither the mechanism by which polarity regulators control cell transformation nor how they interact with oncogenes is well understood.

To directly investigate how polarity proteins regulate breast cancer progression, we examined the effect of deregulating the polarity protein Scribble by itself or in combination with oncogenes HPV E7 and *c-myc*. c-Myc was chosen because it not only regulates initiation and progression of breast cancer, but also

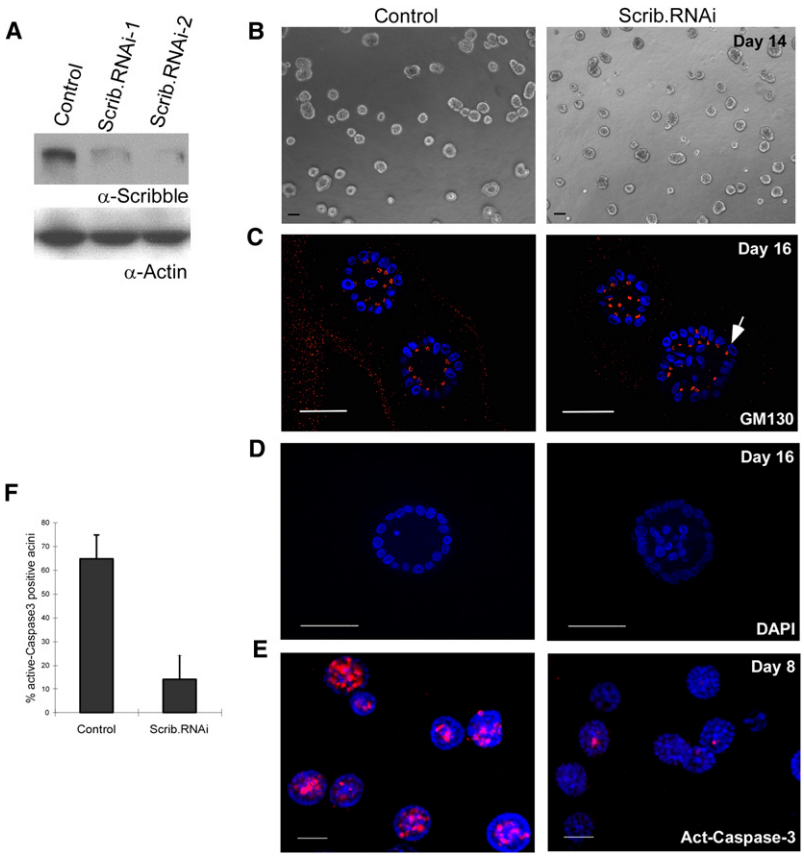

Figure 1. Scribble Loss Blocks Apoptosis and Alters 3D Organization of Epithelial Cells

(A) Scribble expression in stable populations of MCF-10A cells expressing control or independent *scrib* shRNAs.

(B) Phase images of day 14 control or Scrib.RNAi acini.

(C) Golgi orientation was visualized in day 16 acini stained with GM130 (red, Golgi marker) and DAPI. The arrow points to an acinus with a cell where the Golgi is oriented toward the basal surface, which is rarely seen in control acini.

(D) DAPI-stained acini were used to analyze lumen filling.

(E) Control or Scrib.RNAi acini (day 8) immunostained for activated caspase-3 (red, apoptosis marker) and DAPI.

(F) Acini positive for activated caspase-3 were counted and the percentage of the total acini are plotted (n = 3, mean ± SD, > 150 acini/experiment). Scale bar = 50 μM.

lacks the ability to disrupt apical-basal polarity of mammary epithelial cells in culture (Reichmann et al., 1992). The latter property of c-Myc makes it an ideal candidate for investigating interactions between oncogenes and polarity pathways.

Overexpression of *c-myc* is frequently observed in early breast lesions (Spandidos et al., 1987) and the *c-myc* locus is amplified in 15%, of breast tumors (Deming et al., 2000; Liao and Dickson, 2000). Furthermore, c-Myc protein is overexpressed in approximately 70% of breast tumors and correlates with poor clinical prognosis and disease relapse. Although cells in culture and transgenic mouse models have been used to investigate how Myc transforms mammary epithelial cells, the details of the mechanism is not fully understood (Nass and Dickson, 1997; Tilli and Furth, 2003). Expression of c-Myc under the control of mouse mammary tumor virus (MMTV) (Stewart et al., 1984), whey acidic protein (WAP) promoter (Schoenenberger et al., 1988) or under a tetracycline-inducible system (D'Cruz et al., 2001) results in development of mammary tumors with a latency of 7–14 months in 50%–80% of mice. The long latency associated with c-Myc-induced mammary tumorigenesis is likely related to the fact that c-Myc induces both proliferation and apoptosis in mouse mammary epithelial cells in vivo (Nilsson and Cleveland, 2003). Coexpression of c-Myc and growth factors such as transforming growth factor α (TGFα) in transgenic mammary glands shortens the latency by inhibiting apoptosis (Amundadottir et al., 1995; Sandgren et al., 1995). In addition, overexpression of the antiapoptotic protein Bcl2 (Jager et al., 1997), or loss of the proapoptotic protein Bax, cooperates with c-Myc to promote tumorigenesis (Jamerson et al., 2004). These observations demonstrate that inhibition of apoptotic pathways can potentiate c-Myc-induced tumorigenesis in vivo. Neither the mechanisms by which c-Myc induces death in mammary epithelia nor the mechanisms by which the cells develop resistance to c-Myc-induced apoptosis are well understood.

In this study, we demonstrate that deregulation of *scrib* promotes transformation of mammary epithelial cells in vitro and in vivo by disrupting morphogenesis and cell polarity and by inhibiting cell death. We also report that deregulation of *scrib* cooperates with the oncogene *myc* and is selected for during spontaneous mouse mammary tumorigenesis and human breast cancer. These observations have led us to propose a model for investigating the mechanisms by which polarity proteins regulate the initiation of carcinoma in mammals.

RESULTS

Loss of Scribble Disrupts 3D Acinar Morphogenesis of Mammary Epithelial Cells

Although *scrib* expression is frequently lost in breast cancer (Navarro et al., 2005), the significance of this change is not known. To investigate the cellular effects of downregulating *scrib*, we used two different RNA interference (RNAi) constructs to stably deplete *scrib* in the nontumorigenic human mammary epithelial cell line MCF-10A (Figure 1A). Downregulation of *scrib* expression did not induce gross changes in cell morphology and cell-cell junctions as monitored by localization of β-catenin, and F-actin organization (data not shown; see Figure S1A available online). These observations are consistent with previous studies using both MCF-10A cells and canine kidney epithelial cells grown as monolayers (Dow et al., 2007; Qin et al., 2005).

MCF-10A cells, when plated on a bed of extracellular matrix, undergo morphogenesis that involves a proliferative phase (days 1–8) and an apoptotic phase (days 6–9) resulting in formation of proliferation-arrested 3D structures made up of polarized

epithelial cells surrounding a central hollow lumen (Debnath et al., 2002; Muthuswamy et al., 2001). Overall, these 3D acinar structures resemble breast acini in vivo. To determine the role Scribble plays during 3D morphogenesis, Scrib.RNAi cells were plated on a 3D matrix. Scrib.RNAi acini did not show any evidence of hyperproliferation and underwent proliferation arrest, similar to control acini (Figure 1B). To analyze changes in polarity, we monitored the orientation of the Golgi apparatus. In control acini, Golgi were always oriented toward the lumen (Figure 1C and Aranda et al., 2006); however, cells in Scrib.RNAi acini had a modest but reproducible disruption of Golgi orientation, demonstrating that Scribble plays a role during the establishment of apical-basal axis of polarity during acinar morphogenesis. In addition to the modest effect on apical-basal axis of polarity, there was a dramatic effect on the organization of cells within an acinus. The majority of Scrib.RNAi acini (>55%) had cells in the luminal space, whereas we rarely (<6%) observed cells in the lumen of control acini (Figure 1D). Because lumen formation in MCF-10A acini requires apoptosis of centrally located cells (Debnath et al., 2002; Reginato et al., 2005), we investigated whether loss of Scribble inhibited apoptosis. Only 20% of Scrib.RNAi acini showed evidence of luminal cell death as monitored by cleaved caspase-3 staining compared with almost 65% of control acini (Figures 1E and 1F). The shRNA-mediated knockdown was stable throughout the time course of these 3D experiments as validated by the low levels of Scribble in lysates obtained from 24-day-old 3D cultures (Figure S1B). Our results demonstrate that although loss of Scribble had no significant effect on proliferation control, it disrupted normal 3D acinar morphogenesis by inhibiting the establishment of apical-basal polarity and luminal apoptosis.

Loss of Scribble Promotes Abnormal Ductal Morphogenesis in Transgenic Mammary Glands

To determine the effect of Scribble loss on ductal morphogenesis in vivo, we used the mammary fat pad transplantation assay (Edwards, 1996). Previous studies have demonstrated that COMMA-1Dβgeo (CD) cells, an immortalized, pluripotent mouse mammary epithelial cell line derived from a midpregnant BALB/c mouse, efficiently repopulates an epithelium-free (cleared) mammary fat pad by undergoing ductal morphogenesis with primary and secondary branched structures (Aguilar-Cordova et al., 1991; Danielson et al., 1984; Deugnier et al., 2006; Jerry et al., 1994). To demonstrate that CD cells could be used to rapidly generate transgenic mammary glands, CD cells expressing green fluorescent protein (GFP) were transplanted into cleared fat pads. The outgrowths were analyzed 8 weeks after transplantation by imaging freshly isolated mammary fat pads under a fluorescence microscope. Whereas the nontransplanted mammary fat pads did not show evidence of GFP positive ducts (data not shown), fat pads transplanted with CD-GFP cells displayed green ducts (Figure 2A), demonstrating that the cells engineered in culture can repopulate the orthotopic site to form transgenic mammary ducts.

To determine the effect of downregulating Scribble on ductal morphogenesis, CD cells stably depleted of Scribble by RNAi (CD-Scrib.RNAi) (Figure 2B) or the control CD-GFP cells were transplanted into cleared mammary fat pads. At 48 weeks,

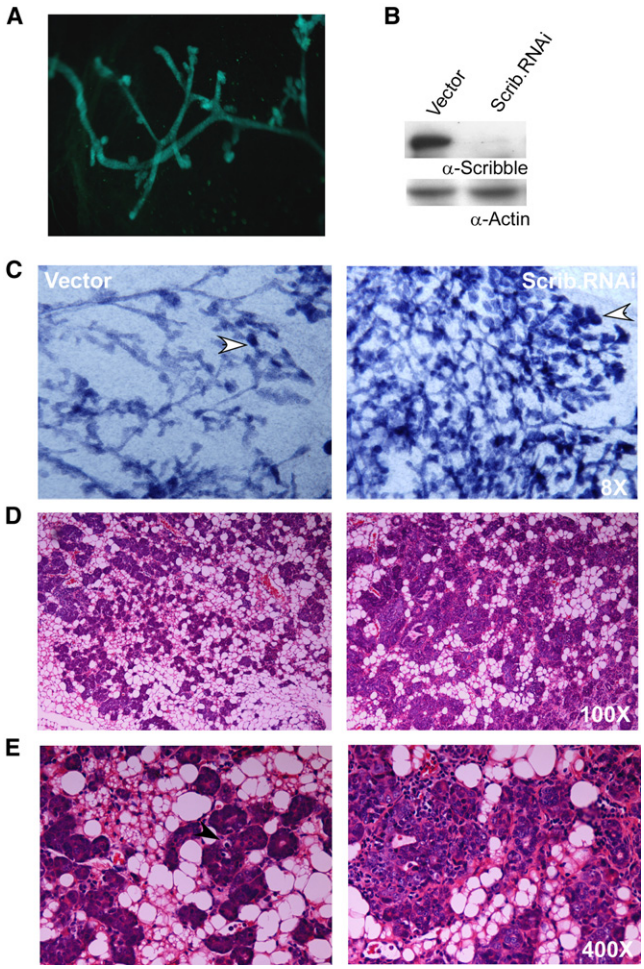

Figure 2. Loss of Scribble Induces Abnormal Morphogenesis in Transgenic Mammary Glands

(A) CD-GFP cells were transplanted into epithelium-free mammary fat pads and imaged by fluorescence microscopy 41 weeks after transplantation.

(B) *scrib* expression in CD cells expressing Scribble.RNAi.

(C) Whole-mount analysis of 41-week-old mammary outgrowth from GFP or Scrib.RNAi cells.

(D) Low-magnification images of H&E-stained sections of CD-GFP or CD-Scrib.RNAi mammary glands.

(E) High-magnification images of H&E-stained sections of CD-GFP or CD-Scrib.RNAi mammary glands.

both GFP and Scrib.RNAi cells repopulated the mammary fat pad with numerous side branches with dense and enlarged end buds (Figure 2C, open arrows). Similar changes were observed within 8 weeks of transplantation (Figure S1C). Histological sections of outgrowths from CD-GFP transplanted glands showed normal glandular structures (Figure 2E, solid arrow). In contrast, the CD-Scrib.RNAi cells formed outgrowths that primarily consisted of multilayered epithelia with no apparent ductal space (Figures 2D and 2E). Over the course of the experiment (48 weeks), 2 of 20 mice (10%) transplanted with CD-Scrib.RNAi cells formed palpable tumors, whereas none of the CD-GFP transplants formed palpable tumors. Histological analysis of the rare tumors suggests that loss of Scribble can result in

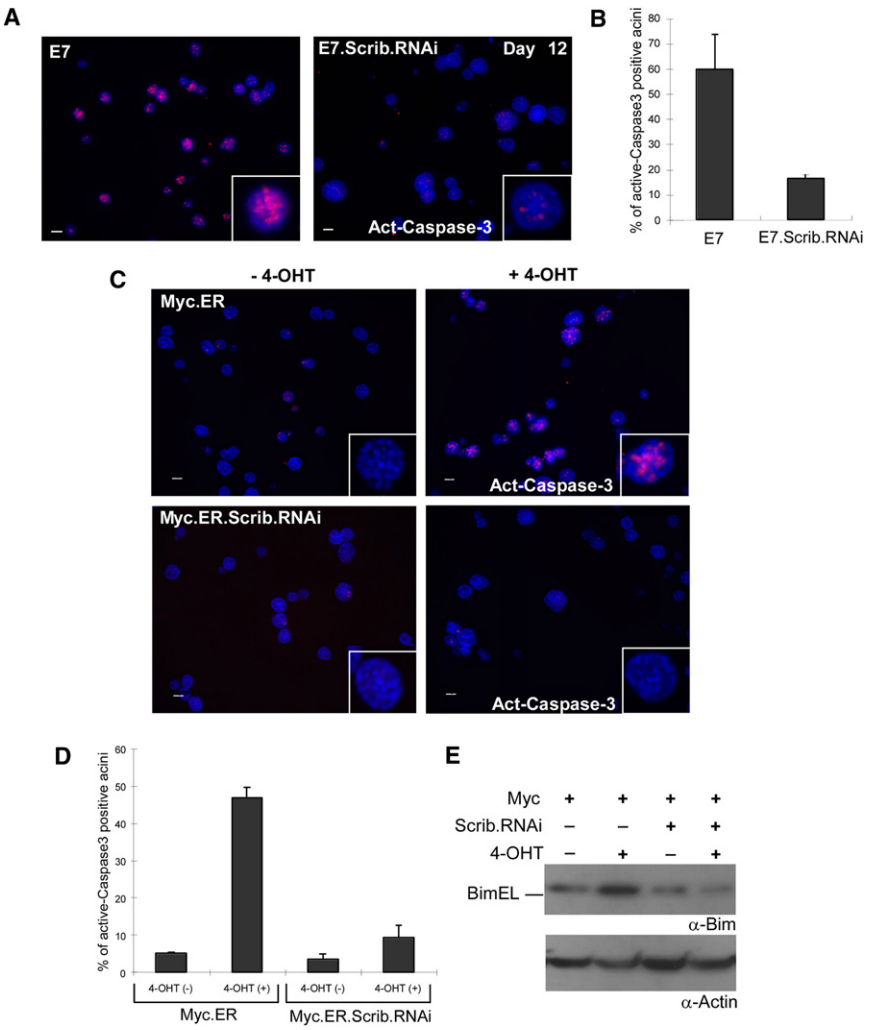

Figure 3. Scribble Loss Blocks Apoptosis in the Context of Myc and E7

(A) Day 8 MCF10A acini expressing HPV16 E7 (E7) alone or in combination with Scribble.RNAi immunostained with activated caspase-3 (red) and DAPI (blue) (10×).

(B) Percentage of activated caspase-3 positive acini from (A) (n = 3, mean ± SD, > 150 acini/experiment).

(C) Acini from MCF10A cells with empty vector (control) or expressing c-Myc fused to estrogen receptor (Myc.ER), with and without Scrib.RNAi, were stimulated (+) on day 2 with 4-OHT and immunostained on day 6 for activated caspase-3 (red) and DNA (blue). Scale bar = 50 μM.

(D) Percent of activated caspase-3 positive acini positive from (C) (n = 3, mean ± SD, > 150 acini/experiment).

(E) Day 8 acini were stimulated with 4-OHT for 12 hr and lysates were analyzed for Bim expression and an actin loading control.

development of glandular, well-differentiated epithelial tumors (data not shown). Thus, cells lacking Scribble are unable to undergo normal epithelial morphogenesis in vivo. In addition, the development of spontaneous tumors in CD-Scrib.RNAi transplants suggests that Scribble functions as a tumor suppressor in mammary epithelial cells.

Loss of Scribble Inhibits Apoptosis Triggered by Activation of Oncogenes in 3D Acini

We have previously demonstrated that HPV E7 expressing MCF-10A acini fail to undergo proliferation arrest (Debnath et al., 2002). However, the increased proliferation was not sufficient to transform acini due to a compensatory increase in apoptosis of cells within the luminal space (Debnath et al., 2002). To investigate the effect of losing Scribble in oncogene-expressing cells, we generated E7-expressing MCF-10A cells deficient in Scribble. Loss of *scrib* expression inhibited apoptosis (Figures 3A and 3B) and resulted in large, filled acini (Figure S2A). Thus, in addition to inhibiting apoptosis during normal 3D acinar morphogenesis, loss of Scribble also blocked apoptosis associated with hyperproliferation triggered by an oncogene, suggesting that Scribble loss might cooperate with oncogenes during transformation.

c-*myc*, an oncogene implicated in breast cancer, induces both proliferation and apoptosis in a number of cell types, including mammary epithelia (Amundadottir et al., 1996; Evan et al., 1992). We investigated whether Myc induces apoptosis in MCF-10A cells and if downregulation of Scribble affects Myc-induced apoptosis. To inducibly activate Myc, we used a Myc-estrogen receptor (ER) fusion protein that can be activated using the estrogen analog 4-hydroxytamoxifen (4-OHT) (Eilers et al., 1989; Littlewood et al., 1995). Stimulation of MCF-10A cells expressing Myc-ER fusion (Figure S2B) induced nuclear translocation of Myc (data not shown), indicating that Myc activation can be induced in these cells. 4-OHT does not have any nonspecific effects on growth and morphogenesis of MCF-10A cells because the cells lack expression of the 4-OHT target, ERα (Lane et al., 1999).

Activation of Myc (for more than 20 days) did not induce apoptosis in cells grown as monolayer cultures with normal levels of serum and growth factors. We next analyzed the effects of Myc activation in cells grown as 3D acini. In the absence of 4-OHT, Myc-ER cells form normal, proliferation-arrested acini by day 12 (data not shown). However, acini grown in the presence of 4-OHT have high rates of cell proliferation (Figure S2C) and increased cell death in each acinus, as monitored by immunostaining for cleaved caspase-3 (Figure S2C). Although c-Myc induced both proliferation and apoptosis in MCF-10A acini, more than 60% of acini died after long-term activation of c-Myc for 28 days (Figures S2D and S2E, see acini with abnormal morphology). These data demonstrate that, unlike cells on plastic dishes, c-Myc induces apoptosis in 3D acini grown in the presence of serum and growth factors. Interestingly, c-Myc-induced

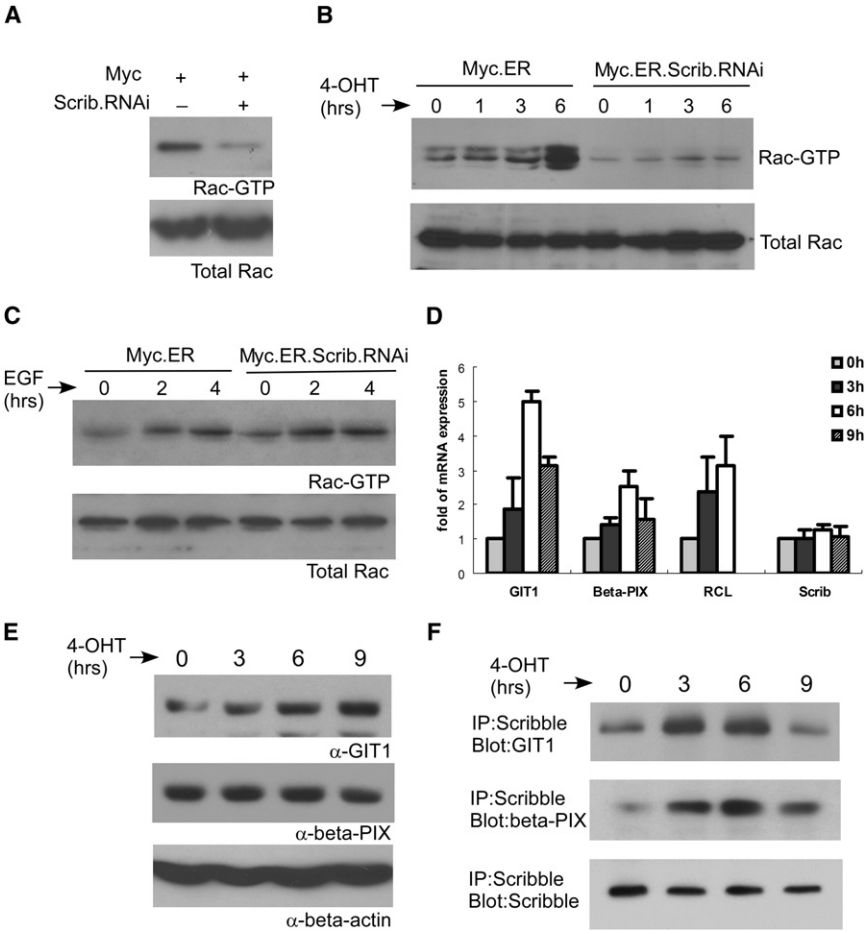

Figure 4. Myc Induces Activation of Rac by Promoting a Scribble-βPIX/GIT1 Interaction

(A) Cell lysates from confluent monolayers grown in the absence of 4-OHT were incubated with GST-PAK1 Rac binding domain and bound Rac (Rac-GTP) was monitored by anti-Rac immunoblots. Total Rac levels were monitored in one tenth of the lysate used for the incubation using anti-Rac immunoblots .

Cell lysates from confluent monolayers stimulated with 4-OHT (B) or EGF (C) for indicated times were used to monitor changes in Rac-GTP levels as in (A).

(D) Cells were stimulated with 4-OHT for indicated times and RNA was isolated. Quantitative PCR was performed using primers against *βpix, rcl*, *gapdh* (glyceraldehyde 3-phosphate dehydrogenase), *git1, scrib*, and *β-actin*. The data were normalized to GAPDH mRNA levels, and fold change in mRNA levels of *βpix, git1, scrib*, and *rcl* is shown. (n = 3, mean ± SD).

(E) Myc.ER cells were stimulated for indicated periods and total cell lysates were analyzed for changes in *GIT1* or *βPIX* protein levels.

(F) Scribble immunoprecipitants were analyzed for coimmunoprecipitated βPIX and GIT1.

apoptosis is dominant over c-Myc-induced proliferation, suggesting that c-Myc-induced transformation of mammary acini is likely to require activation of mechanisms that resist c-Myc-induced apoptosis.

To determine if Scribble loss blocks c-Myc-induced apoptosis, we activated c-Myc in Scrib.RNAi acini. Whereas activation of c-Myc in control acini induced apoptosis in more than 45% of structures, less than 15% of Scrib.RNAi acini showed evidence of cell death in response to c-Myc activation (Figures 3C and 3D). We have previously shown that apoptosis of centrally located cells requires upregulation of Bim, a BH3 domain only proapoptotic protein (Reginato et al., 2005). Consistently, activation of c-Myc induced an increase in the levels of Bim in developing (day 8) 3D structures, and loss of Scribble suppressed the ability of c-Myc to induce Bim expression (Figure 3E). Furthermore, long-term activation of c-Myc in Scrib.RNAi acini resulted in formation of large disorganized multiacinar structures (Figure S3A), suggesting that loss of Scribble can cooperate with c-Myc to transform 3D mammary epithelial structures.

To confirm that these surprising observations are not due to off-target effects of the RNAi approach, we established Myc.ER cells expressing a second *scrib* shRNA and determined that knockdown of Scribble using shRNA-2 phenocopied the effects observed with shRNA-1 (Figure S3B). In addition to using two independent RNAi vectors, we also rescued Scribble expression in Scrib.RNAi cells using an RNAi-resistant cDNA (Figure S4A). The Scribble protein levels reached the pre-RNAi levels as determined by immunofluorescence and the acini with normal levels of Scribble cells became sensitive to Myc-induced apoptosis and upregulated Bim (Figures S4A, S4B, and S4C). Thus, the inhibition of cell death observed in Scrib.RNAi cells is specific to downregulation of Scribble levels and is not due to nonspecific effects of RNAi.

Myc Induces Activation of Rac by Promoting Scribble-βPIX/GIT1 Interaction

Next we investigated the mechanism by which Scribble interacts with c-Myc in mammary epithelial cells. Scribble is a scaffold protein with 16 N-terminal leucine-rich repeats (LRRs) and 4 PSD95/Dlg/ZO-1 (PDZ) domains. Scribble uses its LRRs to localize to the basolateral membranes of polarized epithelial cells and uses its PDZ domains to directly associate with the guanine nucleotide exchange factor (GEF) *ARHGEF7*/βPIX/Cool-1 (Pak-interactive exchange factor beta/cloned-out of library 1) and activate the small GTPases Rac and Cdc42. βPIX is found in a tight complex with G-protein-coupled receptor kinase interactor 1 (GIT1) (Audebert et al., 2004a) and the βPIX-GIT1 complex is known to promote Rac activation at focal adhesions (Frank and Hansen, 2008). To determine if loss of Scribble affected Rac activity in mammary epithelial cells, we monitored the levels of GTP-bound Rac by pulldown assays using the Rac-binding domain of Pak1. Loss of Scribble expression resulted in a significant decrease in Rac-GTP levels (Figure 4A), suggesting that Scribble is a critical regulator of Rac activity in MCF-10A cells.

To investigate the relationship between changes in Rac activity and c-Myc-induced apoptosis, we monitored Rac-GTP levels before and after activation of c-Myc. Surprisingly, activation of c-Myc induced a significant increase in Rac-GTP levels by 6 hr (Figure 4B) and was sustained up to 12 hr (data not shown). Loss of Scribble inhibited c-Myc-induced Rac-GTP loading, suggesting that c-Myc uses Scribble to increase Rac-GTP levels. In contrast, epidermal growth factor (EGF)-induced Rac-GTP loading was not affected by loss of Scribble expression (Figure 4C), demonstrating that Scribble is not required for EGF-induced activation of Rac but is specifically required for c-Myc-induced activation of Rac.

To determine how activation of c-Myc induces Rac activation in a Scribble-dependent manner, we investigated if Scribble itself or members of the Scribble complex are targets of c-Myc-induced transcription. c-Myc, along with its partner Max, binds to DNA with a core consensus sequence of CACGTG (Blackwell et al., 1990, 1993). We reanalyzed data from previously reported genome-wide studies in Burkitt lymphoma cells aimed at identifying genes with promoters that not only have a Myc binding site but also have Myc and Max protein bound to them (Li et al., 2003). Among the members of the Scribble complex, we found that both Myc and Max are bound to the promoter element of βPIX and GIT1 but not Scribble, suggesting that βPIX and GIT1 might be direct transcriptional targets of Myc. Activation of c-Myc in MCF-10A cells induces more than a 2-fold increase in levels of βPIX and GIT1 mRNA (Figure 4D). The increase in the levels of mRNA was similar to or greater than the increase in levels seen for a well-established Myc target, RCL (an N-deoxyribosyltransferase family member) (Figure 4D). As expected, we did not observe any significant change in the mRNA levels of *scrib* (Figure 4D), demonstrating that Myc specifically induces expression of βPIX and GIT1.

To determine if the changes in gene transcription are reflected at the level of composition of the Scribble protein complex, we monitored both changes in protein expression levels of βPIX and GIT1 (Figure 4E) and the formation of the Scribble-βPIX-GIT1 protein complex. Interestingly, activation of Myc induced a significant increase in formation of the Scribble-βPIX-GIT1 trimeric protein complex (Figure 4F), suggesting that Myc directly promotes assembly of the Scribble complex.

Myc Induces Apoptosis by Activating a Rac-JNK–Jun-Bim Pathway

Because activation of JNK, a downstream target of Rac signaling, has been associated with cell death pathways (Kennedy and Davis, 2003), and because JNK activity is required for lumen formation during acinar morphogenesis of mouse mammary epithelial cells (Murtagh et al., 2004), we hypothesized that c-Myc-induced apoptosis in MCF-10A cells might involve Rac-GTP-induced activation of JNK. To determine if c-Myc induced activation of JNK signaling, we monitored the phosphorylation status of a JNK substrate, the transcription factor c-Jun. Activation of c-Myc induced a 5-fold increase in the percentage of control acini positive for phospho-Jun (p-Jun), whereas no significant changes in p-Jun levels were observed in Scrib.RNAi acini (Figures 5A and 5B). Consistent with the IF results, protein lysates derived from 3D acini also showed a c-Myc-induced increase in p-Jun protein levels in a Scribble-dependent manner (Figure 5C), demonstrating that c-Myc activates a Rac-JNK-Jun signaling pathway in MCF-10A cells.

To determine if activation of the Rac-JNK signaling module is required for Myc-induced apoptosis, we inhibited Rac either by expressing a dominant-negative mutant of Rac (RacN17) that potently interferes with Rac signaling or by using a small molecule inhibitor NSC23766, which functions by interfering with the binding between Rac and its GEFs. NSC23766 was shown to specifically inhibit serum-induced Rac but not Rho or Cdc42 activation (Bennett et al., 2001), demonstrating that it is a Rac-specific inhibitor. In addition to inhibiting Rac, we also tested the effect of inhibiting JNK by using the small molecule inhibitor, SP600125, which is known to specifically inhibit the kinase activity of JNK. Inhibition of Rac or JNK potently blocked Myc-induced apoptosis in 3D acini (Figures 5D and S5A), demonstrating that the Rac-JNK signaling is a critical regulator of c-Myc-induced cell death. However, inhibition of mitogen-activated protein kinase kinase did not inhibit c-Myc-induced apoptosis (Figures 5D and S5A), suggesting that c-Myc specifically uses the JNK pathway to induce cell death in polarized mammary epithelial cells. To determine if c-Myc-induced expression of Bim is downstream of the Rac-JNK pathway, we analyzed changes in c-Myc-induced expression of Bim in 3D acini treated with the Rac activation inhibitor NSC23766. Activation of c-Myc did not induce an increase in Bim expression in the presence of NSC23766 (Figure 5E), demonstrating that Rac activation is required for c-Myc-induced changes in Bim expression.

Next we investigated if βPIX is required for c-Myc-induced apoptosis in 3D acini. We downregulated expression of βPIX by RNAi (Figure 5F) and investigated the ability of c-Myc to induce cell death in acini. Downregulation of βPIX phenocopied Scribble loss and blocked c-Myc-induced apoptosis (Figure 5G). Taken together, the above results demonstrate that c-Myc induced cell death in mammary epithelial cells by inducing a Scribble-βPIX/GIT1 complex and activating a Rac-JNK-c-Jun-Bim apoptotic pathway.

Loss of Scribble Cooperates with Myc to Induce Mammary Tumors

To determine whether the c-Myc-Scribble pathway is relevant in a mouse model of human breast cancer, we utilized CD cells and the mammary fat pad transplantation system outlined above (Figure 2). CD cells expressing GFP or Scrib.RNAi were engineered to express c-Myc (without an ER fusion) (Figure 6A). CD-Myc and CD-Myc.Scrib.RNAi cells were transplanted into contralateral glands within the same to animal to avoid interanimal variations (Figure 6B). The formation of palpable mammary tumors was monitored on a weekly basis. Although almost all of the CD-Myc.Scrib.RNAi transplanted mammary glands developed palpable tumors faster than the glands transplanted with CD-Myc cells (9 weeks versus 13 weeks) (Figure 6C), analysis of the tumor onset kinetics for the entire cohort of animals ($n = 19$) did not reach statistical significance ($p = 0.236$). This is consistent with previous reports showing that whereas haploid loss of the proapoptotic gene *bax* cooperated with c-Myc to inhibit apoptosis and promote tumorigenesis, it did not alter the latency of tumors in mice expressing MMTV-Myc (Jamerson et al.,

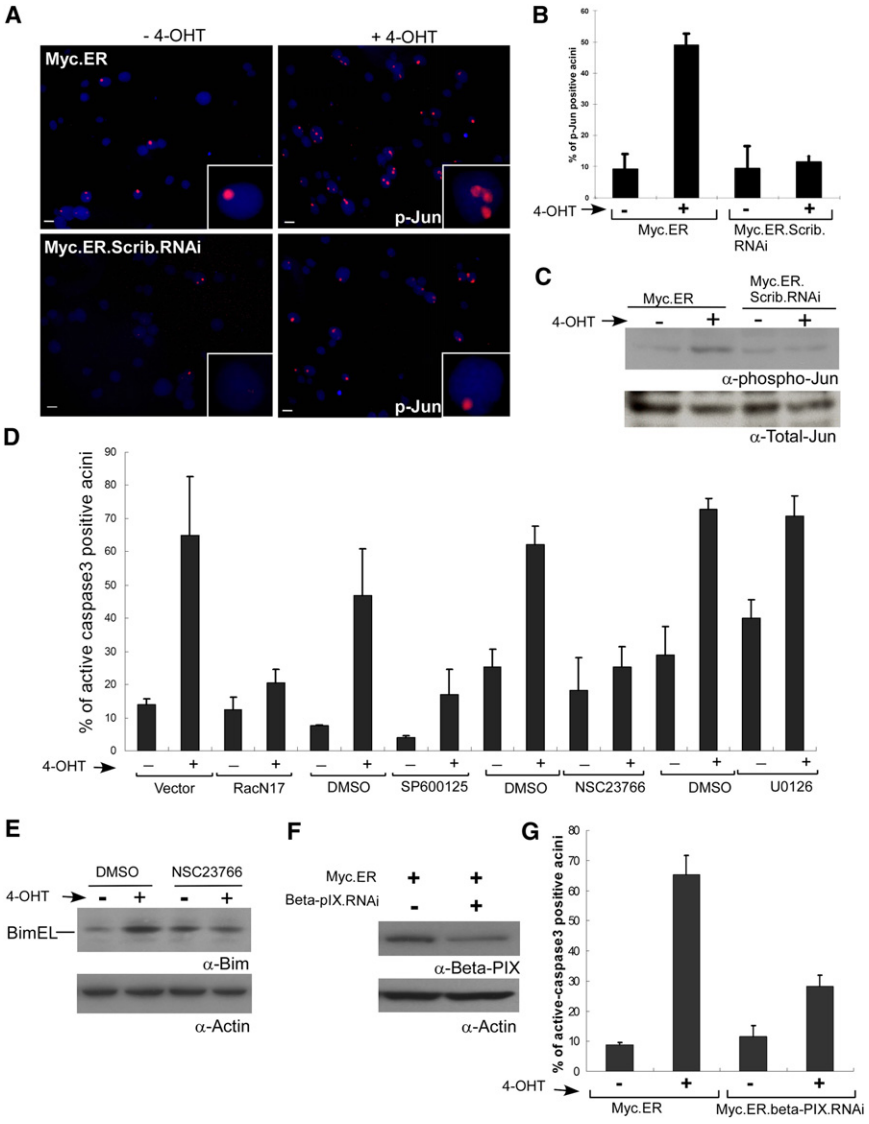

Figure 5. Myc Induces Apoptosis by Activating a Rac-JNK-BIM Pathway

(A) Myc.ER or Myc.ER.Scrib.RNAi acini were stimulated with 4-OHT from days 2–6 and immunostained with p-Jun antibody (red) and with DAPi (blue).

(B) Graph represents quantitation of changes in percentage of p-Jun-positive acini (n = 3, > 100 acini/experiment; mean ± SD).

(C) Protein lysates from acini stimulated for 3 days with 4-OHT and analyzed for changes in p-Jun and total Jun levels.

(D) Percent of activated caspase-3 positive Myc.ER acini (stimulated with 4-OHT from day 2–6) expressing RacN17 (Lentivirally transduced) or treated with JNK inhibitor SP600125 (5 μM), Rac inhibitor NSC23766 (50 mM), or MEK inhibitor U0126 (1.0 μM) (n = 3, mean ± SD, > 150 acini/experiment).

(E) Lysates from Myc.ER acini treated with NSC23766 from day 2–4 and analyzed for changes in BIM-EL levels.

(F) Myc.ER cell populations infected with shRNA targeting the expression of βPIX.

(G) Myc.ER or Myc.ER.β.PIX.RNAi acini were stimulated with 4-OHT and percent of acini positive for activated-casapse-3 was determined (n = 3, mean ± SD, > 150 acini/experiment).

Loss of Scribble Blocks Myc-Induced Apoptosis during Mammary Tumorigenesis

To gain insight into the mechanisms by which loss of Scribble cooperates with c-Myc in vivo, we investigated the apoptosis and proliferation status of the tumors. More than 80% of the cells in CD-Myc tumors stained positive for the apoptosis marker cleaved caspase-3, whereas less than 3% of the cells in CD-Myc.Scrib.RNAi tumors were positive for cleaved caspase-3 (Figure 6G). Similar results were obtained using TUNEL (terminal deoxynucleotidyl transferase biotin-dUTP nick end labeling) apoptosis assay (data not shown). However, both c-Myc and Myc.Scrib.RNAi tumors had similarly high rates of proliferation (Figure 6G), indicating that loss of Scribble does not affect c-Myc-induced proliferation in vivo. Thus, loss of Scribble promotes c-Myc-induced mammary tumorigenesis by inhibiting c-Myc-induced apoptosis and not by enhancing c-Myc-induced proliferation.

We then tested if the Rac-JNK-c-Jun-Bim pathway is active in these c-Myc-induced mammary tumors. All CD-Myc tumors expressed significant levels of Bim (Figure 6H) and p-Jun (Figure 6I), whereas three of the four Myc.Scrib.RNAi tumors expressed low levels of Bim and p-Jun (Figures 6H and 6I). However, one of the four Myc.Scrib.RNAi tumors had high levels of Bim and p-Jun, suggesting that Scribble-independent mechanisms might exist. These observations suggest that c-Myc activates the Rac-JNK-c-Jun-Bim apoptosis pathway in vivo in

2004). However, we observed that the tumors from CD-Myc.Scrib.RNAi cells were almost 10-fold larger than those induced by transplantation of CD-Myc cells (median mass, 0.126 versus 1.236 g) (p = 0.003) (Figures 6B and 6D), indicating that loss of Scribble cooperates with c-Myc in vivo to enhance tumor growth.

Histological analysis of the tumors demonstrated that CD-Myc.Scrib.RNAi cells formed glandular, low grade, and well-differentiated tumors, whereas the CD-Myc cells formed epithelial tumors displaying an apoptotic nuclear morphology (Figure 6E). We found no evidence of lung metastasis during the course of the study, which is consistent with low-grade tumors.

We then investigated whether Scribble loss was maintained throughout the tumorigenic process. Immunoblots of CD-Myc.Scrib.RNAi tumor lysate (all four analyzed) had undetectable levels of Scribble compared to CD-Myc tumors (Figure 6F). Interestingly, one of the four CD-Myc tumors (tumor 3) had lower levels of Scribble than the other tumors analyzed.

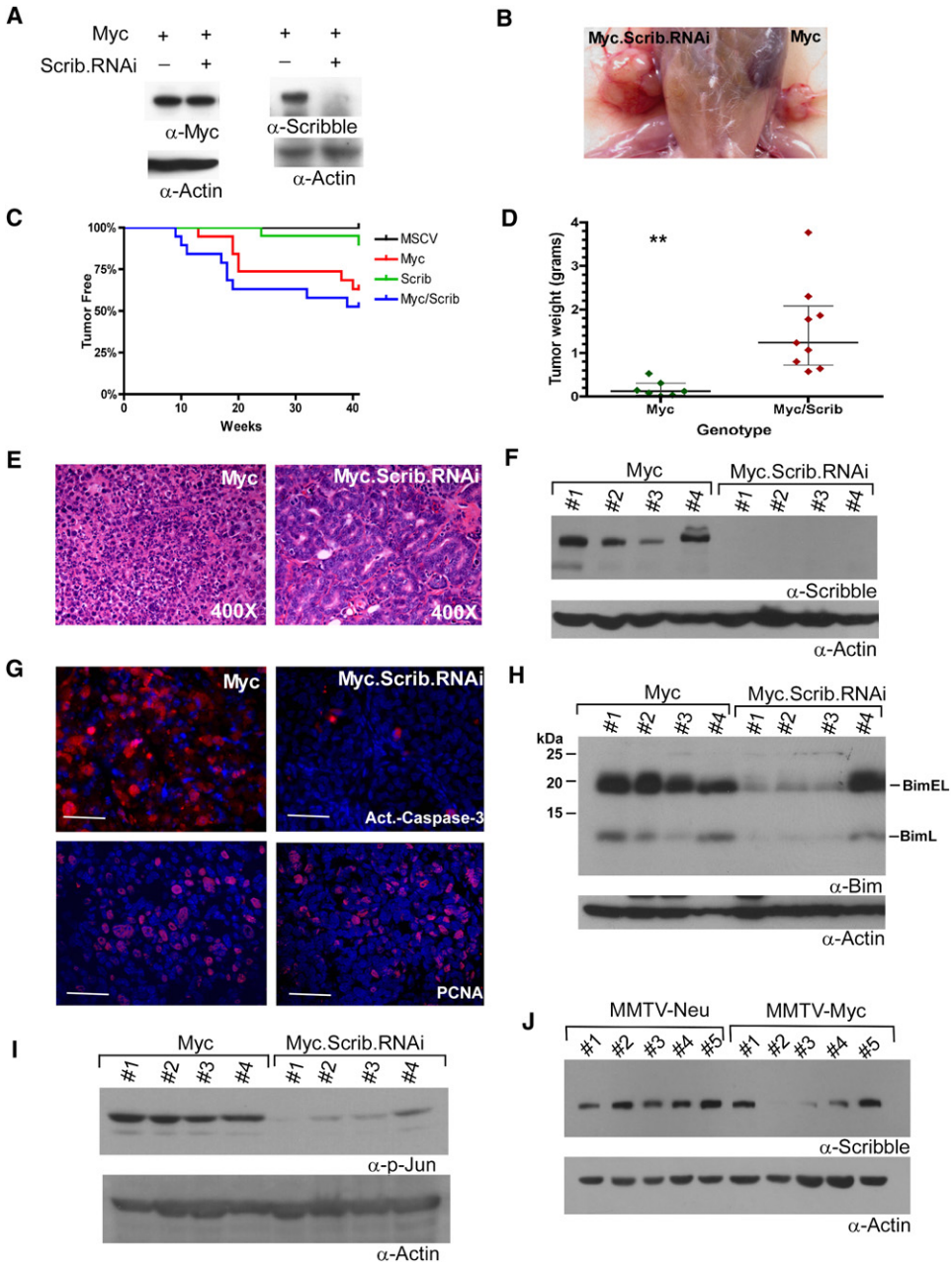

Figure 6. Loss of Scribble Cooperates with Myc to Induce Mammary Tumors

(A) Expression of c-Myc and Scribble in CD.Myc cells alone or in combination with Scrib.RNAi.

(B) Representative mammary tumors in no. 4 and 9 mammary fat pads transplanted with Myc.Scrib.RNAi and Myc cells, respectively, 13 weeks after transplantation.

(C) Kaplan-Meier curve for tumor-free animals transplanted with control (MSCV, n = 20), Myc (n = 19), Scrib.RNAi (n = 20), or Myc.Scrib.RNAi (n = 19).

(D) Myc (n = 7) or Myc.Scrib.RNAi tumors (n = 9) were weighed at the time of isolation and the distribution is plotted. The solid line represents the median value and the interquartile range is indicated. The statistical significance was calculated using a two-tailed t test (p = 0.003).

(E) Tumors were fixed, paraffin embedded, sectioned, and stained with H&E.

(F) Tumors were lysed and Scribble expression was analyzed.

(G) Myc or Myc.Scrib.RNAi tumor tissue was stained by indirect immunofluorescence for activated-caspase-3 (red) or PCNA (red) and DAPI (blue) (n = 3 representative images shown).

Four tumors were analyzed for changes in BIM expression (H) and p-Jun (I) with loading controls.

(J) Protein lysates from spontaneous MMTV-Neu and MMTV-Myc driven mammary tumors were analyzed for changes in levels of Scribble protein expression (actin loading control).

a Scribble-dependent manner and that loss of Scribble blocks the ability of c-Myc to activate the apoptosis pathway.

Loss of Scribble Expression Is Selected for during MMTV-Myc Mammary Tumorigenesis

Next we tested whether Scribble levels are somatically downregulated during the development of mammary tumors in MMTV-Myc transgenic mouse models of human breast cancer. Among the five mammary tumors analyzed from MMTV-Myc tumors (D'Cruz et al., 2001), three had low or undetectable levels of Scribble (Figure 6J), suggesting that loss of Scribble expression is selected for during MMTV-Myc-induced mouse mammary tumorigenesis. By contrast, we did not see any decrease in Scribble levels in any of the four MMTV-HER2/NEU-induced tumors (Guy et al., 1992) (Figure 6J), indicating that downregulation of Scribble is not required or selected for during HER2/NEU-induced tumorigenesis in mice. Thus, there must be a selection pressure to downregulate the expression of Scribble during c-Myc-induced mouse mammary tumorigenesis.

Scribble Is Deregulated by Loss of Membrane Localization in Human Breast Cancer Cell Lines

To determine the relevance to human cancers, we investigated changes in expression of *scrib* in human breast cancer cell lines. Although we did not observe a dramatic decrease in total protein levels, breast cancer cell lines (MCF-7, MDA-MB-231, and SUM159) had Scribble localized to the cytoplasm and not restricted to the cell-cell junctions (Figure 7A and data not shown). This observation raised the possibility that Scribble might also be deregulated by loss of membrane localization. This possibility is consistent with previous findings in *Drosophila* where a single amino acid point mutation in an LRR domain of Scribble mislocalizing it from cell-cell junctions results in a fly phenotype identical to that observed for the *Scrib* complete-loss-of-function mutant (Zeitler et al., 2004). In addition, the mice mutant *rumz*, which results in a defective neuronal migration, was mapped to a *Scrib* allele that harbors a point mutation in the LRR domain (Zarbalis et al., 2004). Together, these results demonstrate that mislocalization of Scribble from cell-cell junctions inactivates the protein in *Drosophila* and mammals.

To directly test whether mislocalization of Scribble deregulates its function in mammary epithelial cells, we mutated a conserved proline at position 305 to a leucine (P305L), which is known to disrupt membrane binding of LRR-domain-containing proteins (Audebert et al., 2004b). We generated Myc.ER cell populations overexpressing either wild-type (WT) Scribble or the P305L mutant. The cells have a modest (2–3-fold) overexpression of Scribble compared with the endogenous levels present in MCF-10A cells (Figure S5B). Immunofluorescence analysis showed that the WT protein localizes to cell-cell junctions whereas the P305L mutant localizes to the cytoplasm, demonstrating that Scribble uses the LRR domain to localize to cell-cell junctions in mammary epithelial cells (Figure 7B). To determine whether mislocalization of Scribble disrupts acinar morphogenesis, day 12 acini were immunostained with GM130 and DAPI (Figure 7C). Whereas the control and WT Scribble-overexpressing cells had a well-developed lumen and polarized Golgi apparatus, P305L acini had no detectable lumen and a disrupted Golgi orientation. Consistently, the P305L-expressing acini did not stain positive for cleaved caspase-3 when compared with control and WT Scribble acini (data not shown). These phenotypes were similar to or more severe than those observed in Scrib.RNAi acini (Figure 1D).

To determine whether mislocalization of Scribble blocks c-Myc-induced cell death, we monitored Myc-induced apoptosis in WT and P305L-expressing cells. Whereas c-Myc induced apoptosis in both control and WT acini, it failed to induce apoptosis in P305L acini (Figure 7D), demonstrating that Scribble mislocalization is sufficient to inhibit c-Myc-induced cell death. These results suggest that the Scribble mislocalization observed in breast cancer cell lines represents a second mode of inactivating Scribble function during cell transformation or tumorigenesis.

Scribble Is Both Downregulated and Mislocalized in Human Breast Cancers

To determine if *scrib* is deregulated in primary human breast cancers, we analyzed both changes in levels of *scrib* mRNA expression and changes in subcellular localization of Scribble. Total RNA was isolated from 32 human tumors and 4 normal breast samples (Figure 7E). Seventeen tumors had more than a 2-fold decrease in the level of *scrib* expression compared with normal breast, as determined by Q-PCR analysis (Figure 7E), suggesting that Scribble levels are frequently downregulated during the evolution of breast tumors.

To determine if Scribble localization was deregulated in primary tumors, both normal and tumor tissues were immunostained with an anti-Scribble antibody. Whereas Scribble was found only at cell-cell junctions of epithelial cells within the TDLU structures of normal breast (Figure 7F), it was mislocalized in 10 of 20 ductal carcinoma in situ (DCIS) samples. However, all the tumors also had regions with normal Scribble localization, demonstrating that tumors are mosaic for normal and mislocalized Scribble. The presence of a mosaic pattern rules out any immunostaining artifacts because the regions with proper cell-cell junction localization serve as an internal control for the immunostaining procedure. In addition, we collected optical sections and determined that Scribble was mislocalized in all sections along the z-axis (data not shown). Thus, Scribble was deregulated by both downregulation and by mislocalization in human breast cancer.

Taken together, our results demonstrate that the polarity protein Scribble is a novel regulator of transformation in mammals. Scribble is deregulated in breast cancer by downregulation or mislocalization, and that the deregulation disrupts polarity and morphogenesis, blocks apoptosis, and cooperates with oncogenes to transform cells in culture and in vivo by regulating the Rac-JNK-c-Jun-Bim pathway (Figure 7G).

DISCUSSION

Disruptions in cell and tissue architecture are observed during initiation and progression of carcinoma. However, neither the mechanism by which cell and tissue architecture is deregulated nor the role tissue architecture plays during cancer is well understood. Our results demonstrate that deregulation of the polarity protein Scribble not only disrupts cell architecture, but also

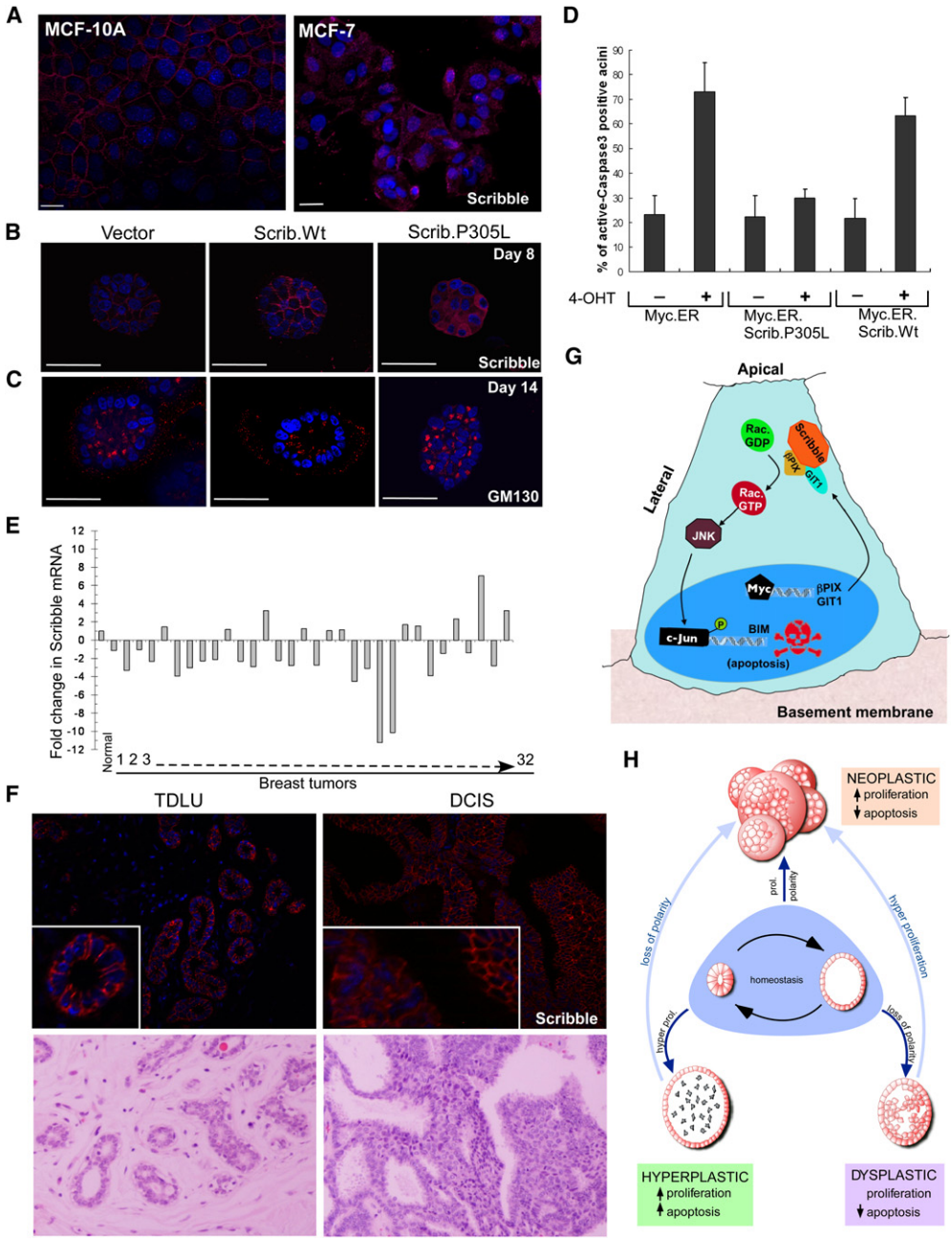

Figure 7. Mislocalization of Scribble Phenocopies Loss of Scribble Expression

(A) MCF-10A and MCF-7 cells on monolayer cultures were immunostained with Scribble (red).

(B) Day 8 Myc.ER acini (vector) or cells expressing wild-type Scribble (Scrib.Wt) or P305L mutant of Scribble (Scrib.P305L) were immunostained with Scribble antibody (red) and DAPI (blue). An optical section through the middle of the acini is shown.

(C) Day 14 acini were immunostained with GM130 (red) and DAPI (blue) and an optical section through the middle of the acini shown.

(D) Percentage of acini that stains positive for activated caspase-3 was determined (n = 3, mean ± SD, > 150 acini/experiment).

(E) RNA isolated from 32 primary human breast tumors and 4 normal breast tissues was analyzed for abundance of Scribble mRNA by quantitative real-time PCR. The graph represents fold change over the average of values obtained from four normal breast samples.

(F) Normal human breast or a DCIS tissue section was immunostained using anti-Scribble antibodies (top panel) and a corresponding section was stained with H&E (lower panel). The inserts show higher-magnification images to highlight changes in Scribble localization.

(G) Summary of the results and a model for how Scribble regulates c-Myc-induced apoptosis in polarized epithelial cells.

(H) A working model for how interaction between cell polarity pathways and oncogenes can be studied within the context of 3D morphogenesis. Remodeling epithelia cycle between proliferation and morphogenesis (indicated by "homeostasis" representing the morphogenesis cycle). Hyperplastic growth is achieved by hyperproliferation without a loss of polarity (e.g., E7) that is coupled to a compensatory increase in apoptosis (gray cells in the lumen). Dysplastic growth is due

functions as a regulator of cell death pathways both during normal morphogenesis and during oncogenesis in vitro and in vivo. Surprisingly, the effects of Scribble knockdown were undetectable in monolayer cultures, suggesting that traditional methods of growing epithelial cells on plastic dishes do not provide the environment to properly study interaction between cell architecture and oncogenic signaling.

Our findings provide novel insight for understanding how cell polarity proteins regulate cell transformation and suggest a working model for understanding the steps leading to initiation of carcinoma. We propose that transformation of epithelial cells should be approached as a deregulated morphogenetic process (Figure 7H) and not just as a simple increase in cell number. Such an approach considers both regulators of cell number and regulators of cell structure as critical components of the oncogenic process. It also accounts for nonpathological increase in cell number observed during normal tissue remodeling that occurs during conditions such as pregnancy and wound repair. Under these normal conditions, the increase in cell number is tightly coupled to a normal morphogenesis program that results in restoration of glandular organization and normal function. Normal epithelial cells are likely to repeat this cell proliferation and morphogenesis cycle throughout life. We refer to this homeostasis as the ''morphogenesis cycle.'' In this context, disruption of polarity pathways induces dysplastic growth by deregulating the morphogenesis cycle without directly affecting cell proliferation, whereas aberrant proliferation signals, in the absence of changes in polarity pathways, induce a simple increase in cell number that results in a hyperplastic state (Figure 7H). A combined deregulation of proliferation and polarity pathways is required to induce the neoplastic growth observed during carcinoma. Thus, investigating transformation of epithelial cells within the context of morphogenesis cycle is likely to provide an ideal platform for better understanding the role played by cell polarity pathways during initiation and progression of carcinoma.

Our results suggest that Scribble regulates spatial control of Rac activation. This is consistent with results showing that Scribble assembles a Cool-1/βPIX-containing complex and facilitates activation of Rac at focal adhesions of migrating epithelia and astrocytes (Dow et al., 2007; Frank and Hansen, 2008; Osmani et al., 2006). In polarized mammary epithelial cells, the P305L Scribble mutant is likely to assemble the βPIX/GIT1 away from cell-cell junctions and therefore interfere with the ability of endogenous Scribble to activate Rac at cell-cell junctions. However, further analysis is required to understand the precise mechanism by which the P305L mutant inhibits the function of WT Scribble. Our results, taken together with those of others, demonstrate that Scribble regulates multiple cellular processes such as cell polarity, directional cell migration, and apoptosis by functioning as a scaffolding protein to activate Rac signaling pathway in a spatially restricted manner.

JNK signaling has been associated with cell death pathways (Kennedy and Davis, 2003); however, a role for the Rac-JNK axis in c-Myc-induced activation of apoptosis was not known. This pathway is likely to be active in multiple cell types because JNK is required for c-Myc to induce apoptosis in Rat1 fibroblasts (Yu et al., 1997). Our results suggest that Bim is a transcriptional target of the Rac-JNK-c-Jun pathway. Consistent with this possibility, studies in neuronal cells show that c-Jun binds directly to the Bim proximal promoter and is required for nerve growth factor withdrawal-induced expression of Bim and apoptosis (Biswas et al., 2007). Our observations also caution the use of JNK inhibitors for treatment of breast cancer. Because inhibition of JNK signaling blocks c-Myc-induced apoptosis, JNK inhibitors could promote growth of tumors that overexpress the *myc* oncogene.

The mechanisms by which cells develop resistance to c-Myc-induced apoptosis is not well understood. Previous studies have shown that the growth factor TGFα inhibits c-Myc-induced apoptosis by inducing expression of Bcl-xL in a AKT and ERK1/2 activation-dependent manner (Amundadottir et al., 1995, 1996; Ramljak et al., 2003). In addition, c-Myc-induced mammary tumors harbor secondary mutations in *Kras2* (D'Cruz et al., 2001), which in turn can activate cell survival pathways. Our results show that disruption of architecture via deregulation of Scribble blocks the ability of c-Myc to trigger apoptosis, identifying a novel mechanism by which cells resist c-Myc-induced apoptosis. A deeper understanding of the interaction between c-Myc and polarity proteins can lead to identification of novel strategies for controlling c-Myc-dependent cancers. Furthermore, regulation of cell death pathways is important for initiation and progression of cancers and plays a critical role during development of resistance to cancer treatments. Thus, further understanding of how polarity pathways are deregulated during transformation will lead to new diagnostic and therapeutic opportunities.

EXPERIMENTAL PROCEDURES

Plasmids

All plasmids, RNAi vectors, and sequences used are detailed in Supplemental Data.

Antibodies and Reagents

Antibodies were purchased from commercial sources and detailed in Supplemental Data. For immunofluorescence, the Scrib antibody was conjugated to Alexa 647 using a fluorophore labeling kit (Molecular Probes). Growth factor reduced Matrigel was used for the 3D culture experiments (BD Transduction Laboratories), as was 4-OHT (Sigma) and SP600125 (Biomol International LP).

Cell Culture

MCF10A cells were cultured as previously described (Debnath et al., 2003). Comma-D β-geo cells were kindly provided by Dan Medina (Baylor College of Medicine) and were maintained as previously described (Deugnier et al., 2006). Populations of MCF-10A cells expressing Myc.ER and/or Scribble.RNAi were generated by retroviral infection of the respective plasmids. Generation of MCF-10A 3D structures, indirect immunofluorescence and biochemical analyses were performed using previously published protocols (Debnath et al., 2003; Xiang and Muthuswamy, 2006). Myc.ER was activated using 1 μM 4-OHT. Populations of Comma-1D cells expressing Myc and/or Scribble RNAi or GFP were generated by retroviral infection and selected with antibiotics as described previously (Muthuswamy et al., 2001).

to a disruption of cell polarity and morphogenesis pathways in the presence of normal proliferation cues. Neoplastic growth is due the combination of hyperproliferation (prol.) and a loss of polarity (polarity)/morphogenesis, which is achieved by two cooperating events, such as Myc and Scribble loss or the activation of strong oncogenes such as ErbB2 and RasV12.

Immunoblotting and Immunofluorescence

Cell lysis, immunoblot analysis, and immunofluorescence analysis were performed as previously outlined (Muthuswamy et al., 2001; Debnath et al., 2003; Xiang and Muthuswamy, 2006).

Rac-GTP Pulldown

Assays were performed using the Rac activation kit (Cell Biolabs) as per the manufacturer's instructions.

Immunoprecipitation

MCF10A Myc ER cells treated for 1, 3, 6, or 9 hr with 1uM 4-OHT or mock treatment were lysed and immunoprecipitation was carried out using 3.0 mg total protein following previously published protocols (Muthuswamy et al., 2001).

Comma-D Transplantation

All transplantation experiments were performed using cells within three or four passages following infection and drug selection. Cells were trypsinized, counted, and resuspended at 100,000 cells/10 μl in RPMI. Three-week-old Balb/C mice were anesthetized and the no. 4 and 9 inguinal mammary fat pads were cleared of endogenous epithelium by removing the tissue between the nipple and the lymph node following established procedures (Ehmann et al., 1987). Then, 100,000 cells in 10 μl RPMI were injected into the epithelium-free fat pad and the incision was closed with sutures. Mice were palpated weekly for tumor onset, starting 1 month after the mammary epithelial cell inoculation. Mice were killed when tumors reached 1.5–2 cm in diameter or, at the latest, 10 months after transplantation. All tumors and glands were weighed. Tumor-free survival was calculated by using the Kaplan-Meier method.

Histological Analysis

Mammary glands or tumors were fixed in freshly prepared 4% paraformaldehyde embedded in paraffin. Five-micrometer sections were used for immunohistochemistry or stained with hematoxylin/eosin (H&E). All tumors were evaluated histologically and all glands that did not produce tumors were evaluated as whole mounts and stained with hematoxylin. The tumor incidences were statistically evaluated using GraphPad Prism (GraphPad Software, Inc., La Jolla, CA).

Tumor Immunoblots

Tumor samples derived from Comma-1D.Myc, Comma-1D.Myc.Scrib.RNAi, MMTV-Myc (gift from L. Chodosh, University of Pennsylvania), and MMTV-ErbB2 were flash frozen in liquid N_2 and were ground by mortar and pestle under liquid N_2 and lysed (as described above) for immunoblotting.

Tumor Immunohistochemistry

Paraffin-embedded mouse and human samples were deparaffinized in xylene twice for 5 min. Antigen retrieval was performed using a pressure cooker to boil the sample in Trilogy for 15 min. Samples were blocked with 10% goat serum in 0.1% Triton:PBS for 1 hr. Staining with cleaved caspase-3, PCNA, or Scribble in blocking buffer was performed in a humidified chamber overnight at 4°C. Samples were incubated with fluorochrome-conjugated secondary antibody for 1 hr at room temperature in blocking buffer and were stained with DAPI.

Real-Time PCR

Total RNA was isolated from MCF10AMyc ER cells stimulated with 1uM 4-OHT for indicated times and from human tissues Versagene RNA tissue Kit (Gentra Systems). The reverse transcription was performed using a probe kit (Applied Biosystems) to generate cDNA and the resulting cDNA was used for PCR using SYBR Green master PCR Mix (Applied Biosystems) in triplicate. The data were gathered on the ABI 7900 sequence detection system. Details on the primers used are provided in Supplemental Materials.

Morphometry

Three-dimensional structure morphology was quantitated using phase images. Briefly, 50–100 3D structures were categorized as normal, disintegrated, or large spheres for two experiments. The percent distribution for each category was calculated and plotted on a graph.

SUPPLEMENTAL DATA

Supplemental Data include Supplemental Experimental Procedures and five figures and are available with this article online at http://www.cell.com/supplemental/S0092-8674(08)01238-5.

ACKNOWLEDGMENTS

We would like to thank Dan Medina (Baylor College of Medicine) for the COMMA-1D cells and for his continued support and guidance during the course of the experiments. We thank Lewis Chodosh for providing tumor samples from MMTV-Myc transgenics and Patrick Humbert for the Scribble cDNA. We also wish to thank Alan Hall and members of the Muthuswamy laboratory for their critical discussions and comments regarding the manuscript, Jim Duffy for his assistance with art work, and Bill Tansey for the reagents and helpful discussions. This work was supported by CA098830, DOD BC075024, and CA105388 grants from NCI, Rita Allen Foundation, FACT foundation, Glen Cove Cares, and Long Islanders Against Breast Cancer.

Received: August 28, 2007
Revised: June 23, 2008
Accepted: September 23, 2008
Published: November 26, 2008

REFERENCES

Aguilar-Cordova, E., Strange, R., Young, L.J., Billy, H.T., Gumerlock, P.H., and Cardiff, R.D. (1991). Viral Ha-ras mediated mammary tumor progression. Oncogene *6*, 1601–1607.

Allred, C.A., Hilsenback, S.G., and Mohsin, S.K. (2004). Biological features of human premalignant breast disease. In Diseases of the Breast, J. Harris, M.E. Lippman, M. Morrow, and K. Osborne, eds. (Philadelphia: Lippincott Williams & Wilkins), pp. 507–520.

Allred, D.C., Mohsin, S.K., and Fuqua, S.A. (2001). Histological and biological evolution of human premalignant breast disease. Endocr. Relat. Cancer *8*, 47–61.

Amundadottir, L.T., Johnson, M.D., Merlino, G., Smith, G.H., and Dickson, R.B. (1995). Synergistic interaction of transforming growth factor alpha and c-myc in mouse mammary and salivary gland tumorigenesis. Cell Growth Differ. *6*, 737–748.

Amundadottir, L.T., Nass, S.J., Berchem, G.J., Johnson, M.D., and Dickson, R.B. (1996). Cooperation of TGF alpha and c-Myc in mouse mammary tumorigenesis: coordinated stimulation of growth and suppression of apoptosis. Oncogene *13*, 757–765.

Aranda, V., Haire, T., Nolan, M.E., Calarco, J.P., Rosenberg, A.Z., Fawcett, J.P., Pawson, T., and Muthuswamy, S.K. (2006). Par6-aPKC uncouples ErbB2 induced disruption of polarized epithelial organization from proliferation control. Nat. Cell Biol. *8*, 1235–1245.

Audebert, S., Navarro, C., Nourry, C., Chasserot-Golaz, S., Lecine, P., Bellaiche, Y., Dupont, J.L., Premont, R.T., Sempere, C., Strub, J.M., et al. (2004a). Mammalian Scribble forms a tight complex with the betaPIX exchange factor. Curr. Biol. *14*, 987–995.

Audebert, S., Navarro, C., Nourry, C., Chasserotgolaz, S., Lecine, P., Bellaiche, Y., Dupont, J., Premont, R., Sempere, C., and Strub, J. (2004b). Mammalian Scribble Forms a Tight Complex with the βPIX Exchange Factor. Curr. Biol. *14*, 987–995.

Bennett, B.L., Sasaki, D.T., Murray, B.W., O'Leary, E.C., Sakata, S.T., Xu, W., Leisten, J.C., Motiwala, A., Pierce, S., Satoh, Y., et al. (2001). SP600125, an anthrapyrazolone inhibitor of Jun N-terminal kinase. Proc. Natl. Acad. Sci. USA *98*, 13681–13686.

Bilder, D. (2004). Epithelial polarity and proliferation control: links from the Drosophila neoplastic tumor suppressors. Genes Dev. *18*, 1909–1925.

Bissell, M.J., Radisky, D.C., Rizki, A., Weaver, V.M., and Petersen, O.W. (2002). The organizing principle: microenvironmental influences in the normal and malignant breast. Differentiation *70*, 537–546.

Biswas, S.C., Shi, Y., Sproul, A., and Greene, L.A. (2007). Pro-apoptotic Bim induction in response to NGF deprivation requires simultaneous activation of three different death signaling pathways. J. Biol. Chem. *282*, 29368–29374.

Blackwell, T.K., Huang, J., Ma, A., Kretzner, L., Alt, F.W., Eisenman, R.N., and Weintraub, H. (1993). Binding of myc proteins to canonical and noncanonical DNA sequences. Mol. Cell. Biol. *13*, 5216–5224.

Blackwell, T.K., Kretzner, L., Blackwood, E.M., Eisenman, R.N., and Weintraub, H. (1990). Sequence-specific DNA binding by the c-Myc protein. Science *250*, 1149–1151.

Bryant, P.J. (1997). Junction genetics. Dev. Genet. *20*, 75–90.

D'Cruz, C.M., Gunther, E.J., Boxer, R.B., Hartman, J.L., Sintasath, L., Moody, S.E., Cox, J.D., Ha, S.I., Belka, G.K., Golant, A., et al. (2001). c-MYC induces mammary tumorigenesis by means of a preferred pathway involving spontaneous Kras2 mutations. Nat. Med. *7*, 235–239.

Danielson, K.G., Oborn, C.J., Durban, E.M., Butel, J.S., and Medina, D. (1984). Epithelial mouse mammary cell line exhibiting normal morphogenesis in vivo and functional differentiation in vitro. Proc. Natl. Acad. Sci. USA *81*, 3756–3760.

Debnath, J., Mills, K.R., Collins, N.L., Reginato, M.J., Muthuswamy, S.K., and Brugge, J.S. (2002). The role of apoptosis in creating and maintaining luminal space within normal and oncogene-expressing mammary acini. Cell *111*, 29–40.

Debnath, J., Muthuswamy, S.K., and Brugge, J.S. (2003). Morphogenesis and oncogenesis of MCF-10A mammary epithelial acini grown in three-dimensional basement membrane cultures. Methods *30*, 256–268.

Deming, S.L., Nass, S.J., Dickson, R.B., and Trock, B.J. (2000). C-myc amplification in breast cancer: a meta-analysis of its occurrence and prognostic relevance. Br. J. Cancer *83*, 1688–1695.

Deugnier, M.A., Faraldo, M.M., Teuliere, J., Thiery, J.P., Medina, D., and Glukhova, M.A. (2006). Isolation of mouse mammary epithelial progenitor cells with basal characteristics from the Comma-Dbeta cell line. Dev. Biol. *293*, 414–425.

Dow, L.E., Kauffman, J.S., Caddy, J., Peterson, A.S., Jane, S.M., Russell, S.M., and Humbert, P.O. (2007). The tumour-suppressor Scribble dictates cell polarity during directed epithelial migration: regulation of Rho GTPase recruitment to the leading edge. Oncogene *26*, 2272–2282.

Edwards, P.A. (1996). Tissue reconstitution, or transgenic mammary gland, technique for modeling breast cancer development. Cancer Treat. Res. *83*, 23–36.

Ehmann, U.K., Guzman, R.C., Osborn, R.C., Young, J.T., Cardiff, R.D., and Nandi, S. (1987). Cultured mouse mammary epithelial cells: normal phenotype after implantation. J. Natl. Cancer Inst. *78*, 751–757.

Eilers, M., Picard, D., Yamamoto, K.R., and Bishop, J.M. (1989). Chimaeras of myc oncoprotein and steroid receptors cause hormone-dependent transformation of cells. Nature *340*, 66–68.

Evan, G.I., Wyllie, A.H., Gilbert, C.S., Littlewood, T.D., Land, H., Brooks, M., Waters, C.M., Penn, L.Z., and Hancock, D.C. (1992). Induction of apoptosis in fibroblasts by c-myc protein. Cell *69*, 119–128.

Frank, S.R., and Hansen, S.H. (2008). The PIX-GIT complex: a G protein signaling cassette in control of cell shape. Semin. Cell Dev. Biol. *19*, 234–244.

Gardiol, D., Kuhne, C., Glaunsinger, B., Lee, S.S., Javier, R., and Banks, L. (1999). Oncogenic human papillomavirus E6 proteins target the discs large tumour suppressor for proteasome-mediated degradation. Oncogene *18*, 5487–5496.

Gardiol, D., Zacchi, A., Petrera, F., Stanta, G., and Banks, L. (2006). Human discs large and scrib are localized at the same regions in colon mucosa and changes in their expression patterns are correlated with loss of tissue architecture during malignant progression. Int. J. Cancer *119*, 1285–1290.

Guy, C.T., Webster, M.A., Schaller, M., Parsons, T.J., Cardiff, R.D., and Muller, W.J. (1992). Expression of the neu proto-oncogene in the mammary epithelium of transgenic mice induces metastatic disease. Proc. Natl. Acad. Sci. USA *89*, 10578–10582.

Humbert, P., Russell, S., and Richardson, H. (2003). Dlg, Scribble and Lgl in cell polarity, cell proliferation and cancer. Bioessays *25*, 542–553.

Jager, R., Herzer, U., Schenkel, J., and Weiher, H. (1997). Overexpression of Bcl-2 inhibits alveolar cell apoptosis during involution and accelerates c-myc-induced tumorigenesis of the mammary gland in transgenic mice. Oncogene *15*, 1787–1795.

Jamerson, M.H., Johnson, M.D., Korsmeyer, S.J., Furth, P.A., and Dickson, R.B. (2004). Bax regulates c-Myc-induced mammary tumour apoptosis but not proliferation in MMTV-c-myc transgenic mice. Br. J. Cancer *91*, 1372–1379.

Jerry, D.J., Medina, D., and Butel, J.S. (1994). p53 mutations in COMMA-D cells. In Vitro Cell. Dev. Biol. Anim. *30A*, 87–89.

Kennedy, N.J., and Davis, R.J. (2003). Role of JNK in tumor development. Cell Cycle *2*, 199–201.

Lane, M.A., Romagnoli, L., Cruise, B., and Cohn, G.M. (1999). Spontaneous conversion to estrogen receptor expression by the human breast epithelial cell line, MCF-10A. Oncol. Rep. *6*, 507–511.

Li, Z., Calcar, S.V., Qu, C., Cavenee, W.K., Zhang, M.Q., and Ren, B. (2003). A global transcriptional regulatory role for c-Myc in Burkitt's lymphoma cells. Proc. Natl. Acad. Sci. USA *100*, 8164–8169.

Liao, D.J., and Dickson, R.B. (2000). c-Myc in breast cancer. Endocr. Relat. Cancer *7*, 143–164.

Littlewood, T.D., Hancock, D.C., Danielian, P.S., Parker, M.G., and Evan, G.I. (1995). A modified oestrogen receptor ligand-binding domain as an improved switch for the regulation of heterologous proteins. Nucleic Acids Res. *23*, 1686–1690.

Lorenzo, C., Mechler, B.M., and Byant, P.J. (1999). What is Drosophila telling us about cancer? Cancer Metastasis Rev. *18*, 295–311.

Macara, I.G. (2004). Parsing the polarity code. Nat. Rev. Mol. Cell Biol. *5*, 220–231.

Margolis, B., and Borg, J.P. (2005). Apicobasal polarity complexes. J. Cell Sci. *118*, 5157–5159.

Murtagh, J., McArdle, E., Gilligan, E., Thornton, L., Furlong, F., and Martin, F. (2004). Organization of mammary epithelial cells into 3D acinar structures requires glucocorticoid and JNK signaling. J. Cell Biol. *166*, 133–143.

Muthuswamy, S.K., Li, D., Lelievre, S., Bissell, M.J., and Brugge, J.S. (2001). ErbB2, but not ErbB1, reinitiates proliferation and induces luminal repopulation in epithelial acini. Nat. Cell Biol. *3*, 785–792.

Nakagawa, S., and Huibregtse, J.M. (2000). Human scribble (Vartul) is targeted for ubiquitin-mediated degradation by the high-risk papillomavirus E6 proteins and the E6AP ubiquitin-protein ligase. Mol. Cell. Biol. *20*, 8244–8253.

Nass, S.J., and Dickson, R.B. (1997). Defining a role for c-Myc in breast tumorigenesis. Breast Cancer Res. Treat. *44*, 1–22.

Navarro, C., Nola, S., Audebert, S., Santoni, M.J., Arsanto, J.P., Ginestier, C., Marchetto, S., Jacquemier, J., Isnardon, D., Le Bivic, A., et al. (2005). Junctional recruitment of mammalian Scribble relies on E-cadherin engagement. Oncogene *24*, 4330–4339.

Nelson, W.J. (2003). Adaptation of core mechanisms to generate cell polarity. Nature *422*, 766–774.

Nilsson, J.A., and Cleveland, J.L. (2003). Myc pathways provoking cell suicide and cancer. Oncogene *22*, 9007–9021.

Osmani, N., Vitale, N., Borg, J.P., and Etienne-Manneville, S. (2006). Scrib controls Cdc42 localization and activity to promote cell polarization during astrocyte migration. Curr. Biol. *16*, 2395–2405.

Qin, Y., Capaldo, C., Gumbiner, B.M., and Macara, I.G. (2005). The mammalian Scribble polarity protein regulates epithelial cell adhesion and migration through E-cadherin. J. Cell Biol. *171*, 1061–1071.

Ramljak, D., Coticchia, C.M., Nishanian, T.G., Saji, M., Ringel, M.D., Conzen, S.D., and Dickson, R.B. (2003). Epidermal growth factor inhibition of c-Myc-mediated apoptosis through Akt and Erk involves Bcl-xL upregulation in mammary epithelial cells. Exp. Cell Res. *287*, 397–410.

Reginato, M.J., Mills, K.R., Becker, E.B., Lynch, D.K., Bonni, A., Muthuswamy, S.K., and Brugge, J.S. (2005). Bim regulation of lumen formation in cultured mammary epithelial acini is targeted by oncogenes. Mol. Cell. Biol. *25*, 4591–4601.

Reichmann, E., Schwarz, H., Deiner, E.M., Leitner, I., Eilers, M., Berger, J., Busslinger, M., and Beug, H. (1992). Activation of an inducible c-FosER fusion protein causes loss of epithelial polarity and triggers epithelial-fibroblastoid cell conversion. Cell *71*, 1103–1116.

Rodriguez-Boulan, E., and Nelson, W.J. (1989). Morphogenesis of the polarized epithelial cell phenotype. Science *245*, 718–725.

Sandgren, E.P., Schroeder, J.A., Qui, T.H., Palmiter, R.D., Brinster, R.L., and Lee, D.C. (1995). Inhibition of mammary gland involution is associated with transforming growth factor alpha but not c-myc-induced tumorigenesis in transgenic mice. Cancer Res. *55*, 3915–3927.

Schoenenberger, C.A., Andres, A.C., Groner, B., van der Valk, M., LeMeur, M., and Gerlinger, P. (1988). Targeted c-myc gene expression in mammary glands of transgenic mice induces mammary tumours with constitutive milk protein gene transcription. EMBO J. *7*, 169–175.

Spandidos, D.A., Pintzas, A., Kakkanas, A., Yiagnisis, M., Mahera, H., Patra, E., and Agnantis, N.J. (1987). Elevated expression of the myc gene in human benign and malignant breast lesions compared to normal tissue. Anticancer Res. *7*, 1299–1304.

Stewart, T.A., Pattengale, P.K., and Leder, P. (1984). Spontaneous mammary adenocarcinomas in transgenic mice that carry and express MTV/myc fusion genes. Cell *38*, 627–637.

Stoll, M., Corneliussen, B., Costello, C.M., Waetzig, G.H., Mellgard, B., Koch, W.A., Rosenstiel, P., Albrecht, M., Croucher, P.J., Seegert, D., et al. (2004). Genetic variation in DLG5 is associated with inflammatory bowel disease. Nat. Genet. *36*, 476–480.

Tilli, M.T., and Furth, P.A. (2003). Conditional mouse models demonstrate oncogene-dependent differences in tumor maintenance and recurrence. Breast Cancer Res. *5*, 202–205.

Xiang, B., and Muthuswamy, S.K. (2006). Using three-dimensional acinar structures for molecular and cell biological assays. Methods Enzymol. *406*, 692–701.

Yu, K., Ravera, C.P., Chen, Y.N., and McMahon, G. (1997). Regulation of Myc-dependent apoptosis by p53, c-Jun N-terminal kinases/stress-activated protein kinases, and Mdm-2. Cell Growth Differ. *8*, 731–742.

Zarbalis, K., May, S.R., Shen, Y., Ekker, M., Rubenstein, J.L.R., and Peterson, A.S. (2004). A focused and efficient genetic screening strategy in the mouse: identification of mutations that disrupt cortical development. PLoS Biol. *2*, E219.

Zeitler, J., Hsu, C.P., Dionne, H., and Bilder, D. (2004). Domains controlling cell polarity and proliferation in the Drosophila tumor suppressor Scribble. J. Cell Biol. *167*, 1137–1146.